Journal Name

COMMUNICATION

Weak backbone CH…O=C and side chain tBu…tBu London interactions help promote helix folding of achiral NtBu peptoids

G. Angelici,[ab] N. Bhattacharjee,[cd] O. Roy,[ab] S. Faure,[ab] C. Didierjean,[e] L. Jouffret,[ab] F. Jolibois,[c] L. Perrin[d]* and C. Taillefumier[ab]
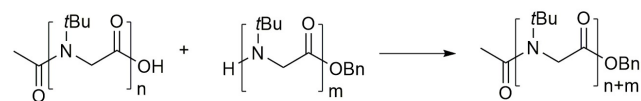
The synthesis of all-*cis* amide (N*t*Bu)-glycine oligomers up to 15 residues long by a blockwise coupling approach is reported. The structure and dynamical behavior of these peptoids have been studied by X-Ray crystallography, NMR and molecular modeling. Analyses unreveal that the folding of these oligomers is driven by weak CH···O=C hydrogen bonding along the peptoid backbone and London interactions between tBu···tBu side-chains.

Peptoids (*N*-substituted glycine oligomers) hold a special place in the foldamer field.[1] On one hand, they are very close mimics of peptides because their main chain is entirely composed of glycine units. On the other hand, the peptoid main chain is deprived of N-H donors and chirality, two main factors that control peptide folding. Additionally, while the amide bond in peptides is preferentially *trans*,[2] peptoid amide bonds populate both *cis* and *trans* conformations. Despite these features, it has been demonstrated that peptoids can adopt discrete secondary structures. Particularly, they have been predicted[3] and shown to adopt the all-*cis* PolyProline-type I (PPI) helical conformation.[4,5] The PPI helical preference is primarily driven by backbone to side chains local interactions of steric and electronic nature. The chiral (*R*) or (*S*)-phenylethyl side chain, which has been used extensively for promoting peptoid PPI-type helices, combines both steric and electronic factors ($n_{c=o(i)}$ to $\pi^*_{Ar(i+1)}$ donation), but fails to provide conformationally homogeneous helices.[6] The triazolium-based side chain was designed for maximizing electronic conformational control.[7] Conversely, the *tert*-butyl side chain,

that was recently reported by us exerts a total *cis* amide control *via* steric effects, independently of the solvent used.[8,9] While short (N*t*Bu) peptoid homo-oligomers are readily prepared by a solution submonomer approach, access to longer oligomers by solid-phase synthesis or solution peptide-type coupling reactions proved to be challenging most likely due to steric hindrance of the (N*t*Bu) glycine units.[8]

Here, we report a convenient access to (N*t*Bu)-oligoglycines with up to 15 residues long, by a blockwise peptide coupling approach and pentafluorophenyl activated ester-based methods (Table 1). As we anticipated that achiral (N*t*Bu) peptoid oligomers could find a special place as foldamers for biomaterial applications, we have studied the structure and the fluxionality of the synthesized homooligomers by (i) X-Ray diffraction, (ii) low temperature NMR and (iii) molecular modeling.

Table 1 Starting acid and amine blocks, and yields of coupling products

Entry	n (Comp.)	m (Comp.)	Coupling reagent	n+m (Comp.)	Yield (%)
1	1 (**1a**)	1 (**1b**)	FDPP[a]	2 (**1**)	60
2	2 (**4**)	2 (**2**)	PFP-O-TFA[b]	4 (**8**)	70
3	6 (**6**)	2 (**2**)	PFP-O-TFA[b]	8 (**9**)	68
4	5 (**5**)	5 (**3**)	PFP-O-TFA[b]	10 (**10**)	73
5	10 (**7**)	5 (**3**)	PFP-O-TFA[b]	15 (**11**)	10
6	10 (**7**)	5 (**3**)	FDPP[a]	15 (**11**)	52

Conditions (a) FDPP (1.2 eq.), DBU (3 eq.), CH₂Cl₂, rt. (b) PFP-O-TFA (1.5 eq.), pyridine (1.5 eq.), CH₂Cl₂, rt.

Preparation of dimer Ac-(N*t*Bu)₂-OBn **1** (Table 1, entry 1 and ESI) was initially chosen as a test synthesis for evaluating a broad range of peptide-type coupling conditions including various carbodiimides, phosphonium, aminium/uronium coupling reagents, the Ghosez's reagent, and pentafluorophenyl diphenylphosphinate (FDPP). Among them, the best result was obtained with FDPP (60% yield) that

a. Université Clermont Auvergne, Université Blaise Pascal, Institut de Chimie de Clermont-Ferrand, BP 10448, F-63000 Clermont-Ferrand, France.
b. CNRS, UMR 6296, ICCF, F-63178 Aubière Cedex, France. E-mail: claude.taillefumier@univ-bpclermont.fr
c. Université de Toulouse-INSA-UPS, LPCNO, CNRS UMR 5215, 135 av. Rangueil, F-31077, Toulouse, France.
d. ICBMS UMR 5246, Université de Lyon, Bât. Curien, 43 Bd. du 11 Novembre 1918, 69622 Villeurbanne, cedex, France. E-mail: lionel.perrin@univ-lyon1.fr
e. LCM3B, Université Henri Poincaré BP 239, Boulevard des Aiguillettes, F- 54509 Vandœuvre les Nancy Cedex France.
Electronic Supplementary Information (ESI) available: [details of any supplementary information available should be included here]. See DOI: 10.1039/x0xx00000x

produces a pentafluorophenyl active ester intermediate whilst most of the other reagents were totally ineffective. It is worth mentioning that FDPP must be used in combination with 3 equivalents of DBU, instead of the weakest bases that only yielded to trace amount of dimer **1**. Later on, we noticed that the easy to handle pentafluorophenyl trifluoroacetate (TFAPfp) furnished similar performance in preparing dimer **1**. Peptoid segments of various sizes (2, 5, 6, and 10 residues in length for the acid blocks, and 2 or 5 residues for the amine blocks) were further coupled efficiently with TFAPfp and/or FDPP as acylating agents (Table 1 and ESI).
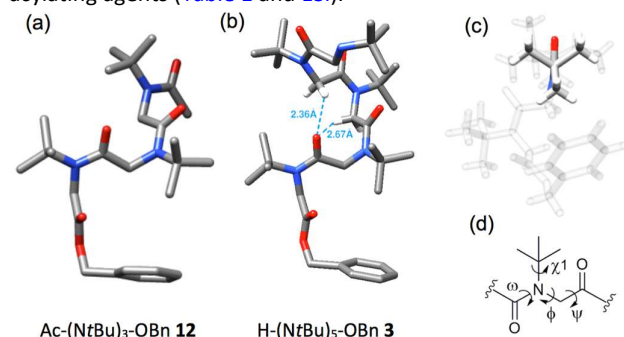

Figure 1 Crystal structures and definition of relevant dihedral angles: (a) X-Ray structure of trimer **12**; (b) X-Ray structure of pentamer **3**; (c) Focus on the amide between residues 1 and 2 in the crystal of **12** showing the typical positioning of the Me groups of the *t*Bu side chains relative to the C=O of residue (*i*-1). (d) dihedral angles: ω [$C_\alpha(i-1)$; $C(i-1)$; N; C_α], ϕ [$C(i-1)$; N; C_α; C], ψ [N; C_α; C; $N(i+1)$], χ_1 [C_α; N; NC_α; C_β]

The X-Ray crystal structure of dimer **1** has been reported recently.[8] Here, we present the crystal structures of trimer Ac-(N*t*Bu)$_3$-OBn **12** and pentamer H-(N*t*Bu)$_5$-OBn **3** obtained from slow evaporation in EtOAc (Fig. 1). As expected, all the amide bonds are *cis*, which provides further confirmation of the remarkable effect of the *t*Bu side chain. The $|\varphi|$ and $|\psi|$ dihedral angles within **12** and **3** lie in a narrow range (68° $< |\varphi| <$ 89° and 162° $< |\psi| <$ 178°, ESI). These values are closed to $|\varphi| \approx 75°$, $|\psi| \approx 170°$ of peptoids adopting a PPI-type helical conformation.[3] They are also in accordance with those of the crystal structure of pentamer H-(N*r*ch)$_5$-NH$_2$ bearing chiral aliphatic cyclohexylethyl side chains.[5] By contrast, the χ_1 side chain torsion angles measured in all the crystallized (N*t*Bu) oligomers differ significantly from those found in peptoids with N-C(α) chiral side chains.[4,5] One of the Me group of the *t*Bu side chain is systematically in close proximity to the backbone methylene group (0° $< |\chi_1| <$ 22°, Fig. 1c and ESI). This eclipsed conformation prevents steric clashes between the two other Me groups and the amide carbonyl group of residue (*i-1*).

Since peptoids are *N*-substituted glycine oligomers, they lack of hydrogen bond donors and hence cannot form conventional CO···HN hydrogen bonds as in peptides. As a consequence, other types of interactions govern peptoids folding. In biological systems, CO···HC carbon-oxygen hydrogen bonds that originate from a Debye interaction are found to be omnipresent and vital for biological structure.[10,11] Recently, inter-annular CH···O hydrogen bonds have been shown to be crucial for the solid-state assembly of peptoid macrocycles.[12] In addition, the attractive London force between bulky aliphatic groups proved to control structures, reactivity and spectroscopy[13] and may have role in the folding of the (N*t*Bu) oligopeptoids under study.

In the X-ray crystal structure of pentamer **3**, two types of weak interactions are captured. Firstly, CO···HC H-bond between the carbonyl group of residue 4 and the backbone methylene hydrogens of residues 3 and 2 are identified, with distances of 2.67 and 2.36 Å shorter than the O···H van der Waals distance (Fig. 1b). Secondly, a *t*Bu···*t*Bu interaction is suggested by the short C(Me):C(Me) distance of 3.92 Å (resp. 4.26 Å) between the *t*Bu groups of residues 1 and 4 (resp. 2 and 5).

Pentamer **3** was optimized using a quantum chemical approach (see ESI for computational details). The superimposition of the backbone of the optimized geometry to the crystal structure of **3** is shown in ESI. The computed Root Mean Squared Deviation (RMSD) of the aligned backbones is 0.4 Å, neglecting the most flexible *C-* and *N*-termini drops it to less than 0.2 Å. The experimental values and signatures of the (φ, ψ) couples of each residue are fairly reproduced by the calculation (ESI, Table S1). This will support further interpretation of the structural analysis and especially the identification of weak interactions within the backbone and between side-chains as discussed in a following section.
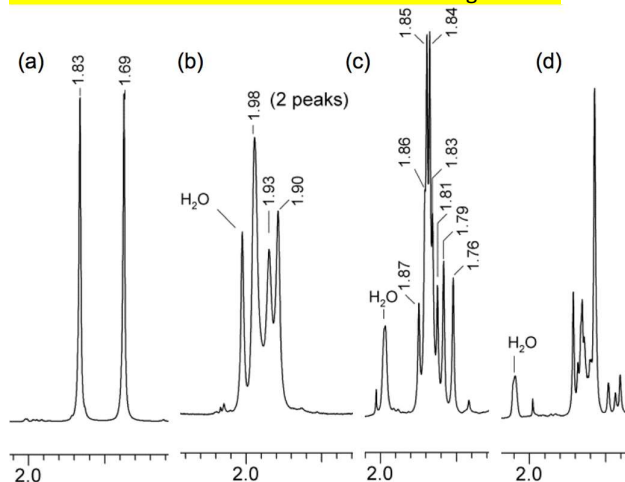

Figure 2. 500 MHz ^{1}H NMR spectra expansions showing methyl acetamide resonances at low temperature: (a) dimer **1** at 200 K in CD$_2$Cl$_2$; (b) trimer **12** at 218 K in CDCl$_3$; (c) tetramer **8** at 200 K in CD$_2$Cl$_2$; (d) pentamer **14** at 200 K in CD$_2$Cl$_2$.

In order to get additional insights in the fluxionality of peptoids bearing *t*Bu side chains, low temperature NMR spectra were recorded for dimer **1**, trimer **12**, tetramer **8**, pentamer **14** and decamer **10**. A rapid equilibrium between several conformations was indeed suggested by the observation of the methyl acetamide group of each oligomer as a broad singlet at room temperature (around 1.90 ppm in CDCl$_3$ or CD$_2$Cl$_2$, ESI). By recording the ^{1}H NMR spectrum of dimer **1**, at 200 K in CD$_2$Cl$_2$, the initial broad signal separated in two singlets of equal intensity suggesting the presence of two conformers close in energy (Fig. 2a). Similarly, the ^{1}H NMR spectrum of trimer **12** shows four broad singlets of close intensity at 218 K in CDCl$_3$ (Fig. 2b) that can be related to four

COMMUNICATION

different conformations. For tetramer **8**, although signals overlap at 200 K, eight peaks of various intensities were attributed to the acetamide methyl group (Fig. 2c). Since, the *t*Bu side chain locks the peptoids amide bonds in the *cis* conformation, and since the ψ angles tend to 180°, we inferred that the conformational variability could originate from different patterns of φ angles. As a result, and in agreement with our observations, an *n*-mer will populate at most 2^{n-1} conformations and also their mirror images that cannot be distinguished by NMR. This is supported by the NMR of pentamer **14** (Fig. 2d) for which a dozens of peaks of uneven intensity, out of the theoretical maximum of 16, are well resolved at 200 K. The same trend was observed for decamer **10**. Although it is difficult to distinguish all the NMR resonances above the tetramer size, some conformations become predominant as the oligomer length increase. This suggests a cooperative effect that has been studied by computational approaches.

In the following, the φ angles will be denoted as +, for +85°, and −, for −85°, for each residue from *N*- to *C*-terminus. From trimer **12** to pentamer **14**, all the possible combinations of φ angles were built and fully optimized at the M06-2X DFT level using an implicit solvent model for dichloromethane (ESI). Among them, in agreement, with the X-Ray experimental data, the $+(-)_n$ (resp. $(+-)_m$) patterns are associated to the most (resp. least) stable structures. The energy difference between the $+(-)_n$ and $(+-)_m$ sequences were calculated from dimer to decamer. Alternate φ angle conformations are higher in energy except for the dimer for which the $(++)_n$ conformer is less stable than $(+-)_m$. The energy gap between the most and least stable conformers does not increase linearly relative to oligomer length (Fig. S1). Peptoids with even number of residues show a dip in the stability gap between $+(-)_n$ and $(+-)_m$. This originates from the formation of a higher amount of weak but favorable CO(*i*)···HC(*i*-1), CO(*i*)···HC(*i*-2), and CO(*i*)···HC(*i*-3) interactions, (see below).

The energetics of a switch of sign of the φ angle was then assessed by performing a relaxed potential energy scan along this dihedral angle from -90° to 90° for the central 4th residue of the $(+)_8$ octamer (Fig. S2). Two minima were found for φ equals 85° and -55° and were fully re-optimized. The most stable conformer is lower in energy by 15.2 kcal mol^{-1} and shows a φ angle of 85°. This value fits with the higher φ angles collected in the X-ray structure of **3** and **12** (see ESI).

The dynamic behavior of the (N*t*Bu) peptoids was scrutinized by molecular dynamics simulations performed for the octamer Ac-(N*t*Bu)$_8$-OBn **9** in an acetonitrile box (ESI). As a control, all simulations were started with the peptoid amide bonds in the *trans* conformation. A shift from *trans* to *cis* was observed over the course of the equilibration.

Analysis of the (φ,ψ) plots of each residue shows that the ψ angle oscillates around ±170°. As the peptoid bonds are locked in *cis*, conformational variability can only arise from the difference of φ angle sign. Production runs performed on $(+-)_4$ or $(+)_8$ did not show any change of sign of φ angle (Fig. S3 and S4). In order to improve the conformational sampling, both $(+)_8$ and $(+-)_4$ conformations were subjected to 50 ns Replica

Exchange Molecular Dynamics (REMD) simulations in the temperature range of 300-600 K.[14] Starting from the $(+)_8$ conformation, only the terminal residues changed of φ angle sign. Starting from $(+-)_4$, the φ angle of all residues were changing sign (Fig. S5 and S6). In conjunction with quantum calculations, the $(+)_n$ conformations turn to be more stable than the alternate $(+-)_m$ ones in REMD simulations.

As several interactions have been pinpointed in the X-ray crystal structure of **3** (Fig. 1b), their probability have been assessed within octamer **9** during 50 ns free MD simulation.

A systematic *ab initio* study has shown that the CO···HC hydrogen bond is less affected by the directionality of the interaction than it's more common CO···HN congener.[15] As a result, the CO···HC interaction only depends on the O···H and C(H)···O distances. A hydrogen bond is counted if the carbon-oxygen distance is less than 3.7 Å and if the hydrogen atom involved in the bonding is at most 2.7 Å away from the oxygen atom.[11] The fraction of simulation time during which a CO(*i*)···HC(*j*) hydrogen bond is formed between the carbonyl oxygen of residue (*i*) with a hydrogen of the methylene backbone of residue (*j*) within both $(+)_8$ and $(+-)_4$ conformations (Fig. 4A). Concerning the London attractive force between *t*Bu side-chains, an interaction has been counted when two methyl carbons of two *t*Bu groups are within 5 Å (Fig. 4B).[13]
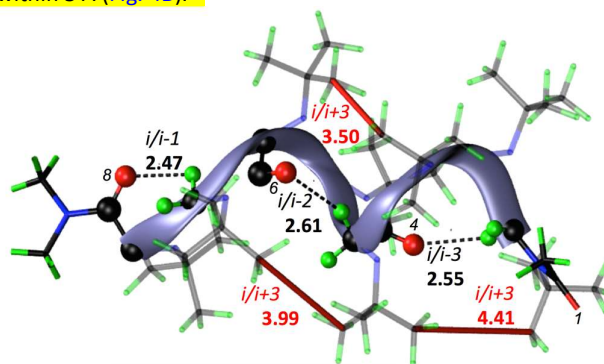

Figure 3 50 ns free MD simulation snapshot of a $(+)_8$ oligopeptoid in which CO···HC (back) i/(i-1), i/(i-2) and i/(i-3) are present simultaneously. i/i+3 interactions between *t*Bu side chain (red) are highlighted the shortest C(Me)···C(Me) distance. Distance are given in Å. Index of residues involved in CO···HC are marked in black italic.

For $(+)_8$, oxygen atoms of the carbonyl groups are involved in H-bonding interactions with the backbone methylene protons up to three residues before, ie *i*/*i*-1, *i*/*i*-2 and *i*/*i*-3. The most occurring interaction is the *i*/*i*-1 (Fig. 3 and 4a). For $(+-)_4$, residue *i* only interacts via H-bonding with residue *i*-1. Concerning the weak attractive interaction between *t*Bu side-chains, $(+)_n$ displays more interactions than $(+-)_4$ (Fig. 4b). In $(+)_n$, the prominent interaction involve *i*/*i*+3 residues. As a consequence, this interaction account for the stability of the $(+)_n$ over the $(+-)_m$ above the tetramer length.

The CO···HC hydrogen bonds are also apparent at the quantum level in the minimized structures of $(+)_8$ and $(+-)_4$. In $(+)_8$, the *i*/*i*-1 interactions are displaced in favor of *i*/*i*-2 and *i*/*i*-3 H-bonds. This is consistent with the X-ray structure of **3** in which the i/i-2 interaction is shorter than the i/i-1 by 0.31 Å. In $(+-)_4$, the optimized geometry displays three i/i-1 interactions

between the carbonyls and the methylene backbone groups. Similarly, the optimized structure of (+)$_8$ shows *t*Bu···*t*Bu interactions captured in MD simulations.
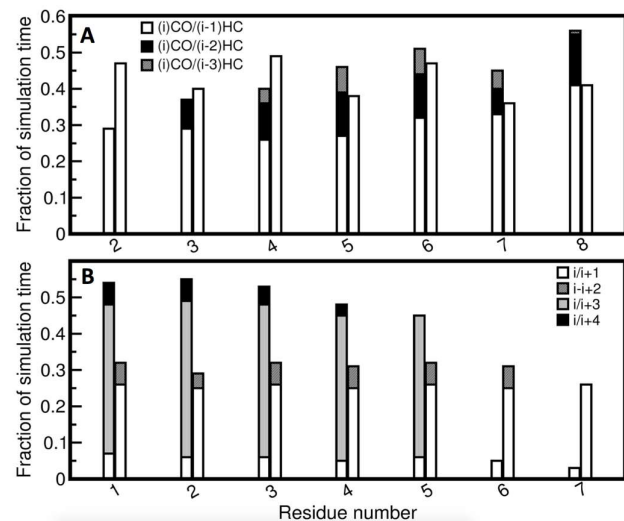

Fig. 4. Fraction of simulation time during which (A) the carbonyl oxygen atom binds a hydrogen atom of the methylene backbone for (+)$_8$ [left bar] and (+-)$_4$ [right bar] oligopeptides (B) two Me of tBu groups interact, for (+)$_8$ [left bar] and (+-)$_4$ [right bar].

Both DFT optimized geometries and MD simulation of (+)$_8$ and (+-)$_4$ octamers reveal CO···HC interactions between the carbonyl oxygen atoms and hydrogen atoms of the *t*Bu side chains. The fraction of simulation time during which this hydrogen bond is formed has been estimated (Fig. S7 and S8). In contrast to the *i*/(*i*-1) contact previously reported,[16] hydrogen bonds develop within the same residue and between CO(*i*) and *t*Bu CH(*i*+1) in (+)$_8$. A similar trend of interactions is found in (+-)$_4$. In this case, additional interactions between the carbonyl group of residue *i* and the side chain of residue *i*-1 are also identified but to a lesser extent than the *i*/*i*+1 (ESI). The similarity of the carbonyl to side chain H-bond interactions for the (+)$_8$ and (+-)$_4$ conformers infer that, although this interaction account for the overall stability of the N*t*Bu peptoids, it does not account for the stability of the (+)$_n$ conformation over the (+-)$_m$.

The stabilization of the (+)$_n$ conformers over the others originates from the H-bond network that is formed along the backbone between residues i/i-1, i/i-2 and i/i-3. In Conclusion, the strength of this network is cumulative with the number of residues and explains the excess of population of some rotamers observed above the tetramer length. This network, which is described for the first time, seems to be specific of the *t*Bu side chain. It might be related to the χ_1 angle that tends to 0° (modulo 120°) and a more open φ angles (85° instead of 75° on average) that are both characteristic of the *t*Bu side chain. Remarkably, by stabilizing the (+)$_n$ sequence, both the CO(*i*)···HC(*i*-n) (n= 1, 2, 3) backbone H-bond network and *i*/*i*+3 *t*Bu···*t*Bu London interactions allow achiral peptoids to adopt preferentially the PPI-like helical conformation.

Notes and references

1 (a) R. J. Simon, R. S. Kania, R. N. Zuckermann, V. D. Huebner, D. A. Jewell, S. Banville, S. Ng, L. Wang, S. Rosenberg, D. C. Spellmeyer, R. Tan, A. D. Frankel, D. V. Santi, F. E. Cohen, and P. A. Bartlett, *Proc. Natl. Acad. Sci. USA*, 1992, **89**, 9367; (b) W. S. Horne, *Expert Opin. Drug. Discov.,* 2011, **6**, 1247.

2 (a) D. E. Stewart, A. Sarkar and J. E. Wampler, *J. Mol. Biol.,* 1990, **214**, 253; D. Pal and P. Chakrabarti *J. Mol. Biol.,* 1999, **294**, 271; (b) A. Jabs, M. S. Weiss and R. Hilgenfeld, *J. Mol. Biol.,* 1999, **286**, 291.

3 P. Armand, K. Kirshenbaum, A. Falicov, R. L. Dunbrack Jr, K. A. Dill, R. N. Zuckermann, and F. E. Cohen, *Fold. Des.*, 1997, **2**, 369.

4 J. R. Stringer, J. A. Crapster, I. A. Guzei, and H. E. Blackwell, *J. Am. Chem. Soc.*, 2011, **133**, 15559.

5 C. W. Wu, K. Kirshenbaum, T. J. Sanborn, J. A. Patch, K. Huang, K. A. Dill, R. N. Zuckermann, and A. E. Barron, J. Am. Chem. Soc., 2003, 125, 13525.

6 (a) P. Armand, K. Kirshenbaum, R. A. Goldsmith, S. Farr-Jones, A. E. Barron, K. T. V. Truong, K. A. Dill, D. F. Mierke, F. E. Cohen, R. N. Zuckermann, and E. K. Bradley, *Proc. Natl. Acad. Sci. U.SA*, 1998, **95**, 4309; (b) C. W. Wu, T. J. Sanborn, K. Huang, R. N. Zuckermann, and A. E. Barron, *J. Am. Chem. Soc.*, 2001, **123**, 6778; (c) C. W. Wu, T. J. Sanborn, R. N. Zuckermann, and A. E. Barron, *J. Am. Chem. Soc.*, 2001, **123**, 2958; (d) S. Mukherjee, G. Zhou, C. Michel, and V. A. Voelz, *J. Phys. Chem. B*, 2015, **119**, 15407.

7 C. Caumes, O. Roy, S. Faure, and C. Taillefumier, *J. Am. Chem. Soc.*, 2012, **134**, 9553.

8 O. Roy, C. Caumes, Y. Esvan, C. Didierjean, S. Faure, and C. Taillefumier, *Org. Lett.*, 2013, **15**, 2246.

9 (a) T. Hjelmgaard, S. Faure, E. De Santis, D. Staerk, B. D. Alexander, A. A. Edwards, C. Taillefumier, and J. Nielsen, *Tetrahedron*, 2012, **68**, 4444; (b) T. Hjelmgaard and J. Nielsen, *Eur. J. Org. Chem.*, 2013, 3574.

10 S. Scheiner, *Phys. Chem. Chem. Phys.*, 2011, **13**, 13860.

11 S. Horowitz, and R. C. Trievel, *J. Biol. Chem.*, 2012, 287, 41576.

12 C. Tedesco, L. Erra, I. Izzo, and F. De Riccardis, *Cryst. Eng. Comm.*, 2014, **16**, 3667.

13 J. P. Wagner, and P. R. Schreiner, *Angew. Chem. Int. Ed. Engl.*, 2015, **54**, 12274.

14 G. L. Butterfoss, B. Yoo, J. N. Jaworski, I. Chorny, K. A. Dill, R. N. Zuckermann, R. Bonneau, K. Kirshenbaum, and V. A. Voelz, *Proc. Nad. Acad. Sci. USA*, 2012, 109, 14320.

15 Y. Gu, T. Kar, and S. Scheiner *J. Am. Chem. Soc.*, 1999, **121**, 9411.

16 F. S. Nandel, R. R. Jaswal, A. Saini, V. Nandel and M. Shafique: *J. Mol. Model.,* 2014, **20**, 2429.